



Identification of candidate diagnostic and prognostic biomarkers for human prostate cancer: RPL22L1 and RPS21

Zumu Liang¹ · Qingjie Mou² · Zhiwei Pan³ · Qiang Zhang¹ · Guojun Gao⁴ · Yingying Cao² · Zhiqin Gao¹ · Zhifang Pan¹ · Weiguo Feng¹

Received: 27 March 2019 / Accepted: 7 May 2019 / Published online: 14 May 2019
© Springer Science+Business Media, LLC, part of Springer Nature 2019

Abstract

Prostate cancer (PCa) is one of the most common malignancies in men worldwide. This study was designed to investigate the potential of Ribosomal Protein L22-like1 (RPL22L1) and Ribosomal Protein S21 (RPS21) as diagnostic and prognostic biomarkers for PCa. First, RPL22L1 and RPS21 were screened as the key molecular of PCa by bioinformatics analysis. Subsequently, the prostate tissue samples were stained for antibodies against RPL22L1 and RPS21. The unbiased signal quantification was performed by ImageJ software, and the results showed that the expression of RPL22L1 and RPS21 exhibited significant differences between the PCa tissues and the normal prostate tissues. Receiver-operating characteristics (ROC) curves were prepared, and then the area under the curve (AUC) values of RPL22L1 and RPS21 were calculated as 0.798 and 0.768, and the likelihood ratio (LR) values of RPL22L1 and RPS21 were calculated as 2.86 and 2.53. These data implied that the over-expression of RPL22L1 and RPS21 is associated with the presence of PCa. The further analysis suggested that the expression of RPL22L1 and RPS21 were significantly higher in high Gleason grade than they were in low Gleason grade. In addition, in vitro studies were undertaken to evaluate the roles of RPL22L1 and RPS21 in PCa. The results revealed that these genes promote PCa cell proliferation, migration and invasion, and inhibit PCa cell apoptosis. Taken together, these data showed that RPL22L1 and RPS21 exhibited higher expression in human prostate cancer tissue, and involved in PCa cell proliferation and invasion. This research provided a novel insight into diagnostic and prognostic biomarkers for PCa.

Keywords RPL22L1 · RPS21 · Prostate cancer · Biomarker · Expression

Introduction

Prostate cancer (PCa) is one of the most common malignancies in men worldwide, and its incidence rate increased continuously in recent years [1–3]. It was estimated that over 160,000 new cases were diagnosed in USA in 2017 [4]. Therefore, early diagnosis is pivotal for the treatment of PCa. At present, PSA has been used as a biomarker for PCa diagnosis [5], however, this modality has numerous drawbacks. For example, the specificity is low, when PSA is moderately elevated [6, 7]. Consequently, it is necessary to identify more specific biomarkers for PCa.

An increase of ribosome biogenesis is a key feature of cell proliferation [8]. Accumulated evidence demonstrated that the dysregulated ribosome biogenesis played an important role in the tumorigenesis [9] including brain [10], esophagus [11] and breast cancer [12]. These researches suggested a relation between the tumor and the over-expression of ribosomal proteins. Ribosomal Protein L22-like1 (RPL22L1)

Zumu Liang, Qingjie Mou and Zhiwei Pan are Co-first authors.

✉ Zhifang Pan
sdwfpzf@126.com

✉ Weiguo Feng
fengwg@wfmcc.edu.cn

¹ College of Bioscience and Technology, Weifang Medical University, NO 7166, Baotong ST, Weifang City 261053, People's Republic of China

² College of Clinical Medical, Weifang Medical University, Weifang, People's Republic of China

³ Laizhou Development Zone Hospital, Yantai, People's Republic of China

⁴ Affiliated Hospital of Weifang Medical University, Weifang, People's Republic of China

and Ribosomal Protein S21 (RPS21) are components of the ribosomal subunit. However, there are very few studies on the relationship between the RPL22L1 and RPS21 expression and PCa.

In this study, we screened RPL22L1 and RPS21 as the key molecular of PCa by bioinformatics analysis, and then analyzed the relationship between their expression and PCa using the quantitative approach. Moreover, *in vitro* studies were conducted to evaluate the roles of RPL22L1 and RPS21 in PCa cell proliferation, invasion and apoptosis.

Materials and methods

Tissue samples

The tissue microarrays were obtained from Alenabio Co.Ltd (Xian, China) including 85 PCa samples and 42 normal prostate tissue samples.

Bioinformatics analysis

In our previous research, RPL22L1 and RPS21 were screened as hub genes involved in PCa according to bioinformatics analysis [13]. In this study, Gene Expression Profiling Interactive Analysis (GEPIA) online tool (<http://gepia.cancer-pku.cn/>) was used to further verify the expression and correlation of genes. Search Tool for the Retrieval of Interacting Genes (STRING) (<https://string-db.org/cgi/input.pl>) database was applied to confirm the protein–protein interaction between RPL22L1 and RPS21.

Immunohistochemistry of RPL22L1 and RPS21

Immunohistochemistry (IHC) was performed as previous research [14]. The tissue samples were pre-treated using 0.3% H₂O₂ and blocked using 10% bovine serum albumin (BSA) for 30 min. Subsequently, the tissue samples were incubated overnight with anti-RPL22L1 and anti-RPS21 (Proteintech, Wuhan, China, 1:200 dilution) at 4 °C and then incubated with secondary antibody (Beyotime, Shanghai, China, 1:2000 dilution) for 2 h at room temperature. Finally, 3,3-diaminobenzidine (DAB) was used for color visualization and hematoxylin was used for counterstained. In addition, primary antibody was replaced by IgG (Santa Cruz, CA, USA, 1:200 dilution) for negative control in this study.

Signal quantification and analysis

ImageJ software was used to perform the unbiased signal quantification as previous study [15]. The high resolution images of tissue samples were analyzed as follows: open ImageJ, open image, invert image, convert image to 16 bit,

convert image to mask, analyze particles (Size 0.5–Infinity, Circularity 0.00–1.00) and then save the images [16]. Then, the particle data were incorporated into Graphpad Prism software, and the area fraction (AF) was calculated to test the significance of difference between the PCa and normal groups. Meanwhile, the Receiver Operating Characteristics (ROC) curves were created by Graphpad Prism software, and the area under the curve (AUC) and the likelihood ratio (LR) were calculated. Additionally, box plots were constructed by Graphpad Prism software to illustrate the expression changes with Gleason grade of PCa.

Cell culture and lentivirus transfection

Human cell lines (DU145 and PC3) were obtained from Chinese Academy of Sciences Cell Bank (Shanghai, China). The cells were cultured in Dulbecco's modified Eagle's medium (DMEM; Invitrogen, Shanghai, China) supplemented with 10% fetal bovine serum (FBS; Gibco, Shanghai, China). The lentiviral mediated RNA interference targeting RPL22L1/RPS21 were constructed by Sangon biotech (Shanghai, China), which were transfected into PC3 cells to knockdown the expression of RPL22L1 and RPS21. Finally, the stable cell lines shRPL22L1/RPS21-PC3 were obtained by puromycin (1 µg/mL) selection.

Western blot

Western blot was performed as previous study [17]. Briefly, the protein was subjected to SDS-PAGE and then transferred to PVDF membranes (Beyotime, Shanghai, China), and incubated with anti-RPL22L1 (Proteintech, Wuhan, China, 1:1000 dilution), anti-RPS21 (Proteintech, Wuhan, China, 1:1000 dilution) and anti-β-actin (Beyotime, Shanghai, China, 1:1000 dilution). After washing, the membranes were incubated with secondary antibody (Beyotime, Shanghai, China, 1:5000 dilution). At last, the bands were analyzed by the enhanced chemiluminescence reaction kit (ECL; Beyotime, Shanghai, China).

Cell proliferation and colony formation

The PC3 cells were grown in 96-well plates, and cell proliferation was monitored using the CCK-8 kit (Beyotime, Shanghai, China) according to the manufacturer's instructions. Colony formation was examined 2 weeks after seeding 200 PC3 cells per well in 6-well plates as previous study [18].

Wound-healing and invasion assays

The wound-healing assay was performed as previous study [19]. PC3 cells were cultured in serum-free medium, and

then the cell-free gaps of 500 μm were created by micropipette tip. The migration cell areas were photographed using microscope (Olympus, Tokyo, Japan) after 24 h. The invasion assay was performed according to the method previously described [20]. PC3 cells were seeded into Matrigel-coated transwell chambers (Sigma-Aldrich, St. Louis, MO, USA) for 24 h, and then the cells that passed through the membrane were counted.

Cell apoptosis assay

The cell apoptosis was detected by the Annexin V-FITC apoptosis detection kit (BD biosciences, San Jose, CA, USA) according to the manufacturer's instructions, and analyzed with a flow cytometer (FACScan) as previous study [2].

Statistical analysis

Statistical analyses were performed by SPSS 19.0 software (IL, USA). Independent sample *t* tests or ANOVA test were used to compare the continuous variables between the two groups or more than two groups. All experiments were performed in triplicate. Data were expressed as mean \pm SE, and $P < 0.05$ was considered as significantly different.

Results

Analysis of RPL22L1 and RPS21 by bioinformatics tool

RPL22L1 and RPS21 were analyzed by GEPIA and STRING database. The result from GEPIA analysis suggested that the expression of RPL22L1 and RPS21 were upregulated in PCa tissues than the normal prostate tissues (Fig. 1a, b), and the expression of RPL22L1 was positively correlated with the expression of RPS21 (Fig. 1c). The result of STRING analysis showed that protein–protein interaction existed between RPL22L1 and RPS21 (Fig. 1d). Combined with our previous study [13], these results indicated that RPL22L1 and RPS21 might be key molecular of PCa.

Signal quantification and analysis

To validate the bioinformatics analysis data, the expression of RPL22L1 and RPS21 were examined by IHC in PCa tissues and the normal prostate tissues. As shown in Fig. 2, the expression of RPL22L1 and RPS21 were significantly upregulated in the cancer cells from the tumor tissues compared with the normal tissues. Additionally, the staining results showed that RPL22L1 was located in cytoplasm and nucleus, while RPS21 was located in cytoplasm. Based on GEPIA database, co-expression analysis indicated that

RPL22L1 and RPS21 expression were positively correlated with other commonly used markers such as PCA3 ($P < 0.05$, data not shown). Subsequently, quantitative ImageJ analysis of RPL22L1 and RPS21 expression were performed, and then the results were incorporated into Mountain plots. Red represented the PCa cores and green represented the normal prostate cores. The results indicated that RPL22L1 and RPS21 exhibited predominant differences between the tumor tissues and the normal tissues (Fig. 3, $P < 0.0001$).

Expression of RPL22L1 and RPS21 to create ROC curve

To assess the potential efficiency of RPL22L1 and RPS21 as biomarker, ROC curves were prepared, and then the area under the curve (AUC) and the likelihood ratio (LR) were calculated (Fig. 4). AUC values of RPL22L1 and RPS21 were 0.798 and 0.768, and LR values of RPL22L1 and RPS21 were 2.86 and 2.53. These data indicated that RPL22L1 and RPS21 might be potential biomarker for PCa.

Changes in expression of RPL22L1 and RPS21 with Gleason grade

Changes in expression of RPL22L1 and RPS21 were analyzed between the high and low Gleason grade of PCa (Fig. 5). The expression of RPL22L1 was significantly higher in Gleason grade 8 than it was in Gleason grade 5 ($P < 0.05$). Likewise, the expression of RPS21 increased significantly in Gleason grade 8 compared with Gleason grade 5 and Gleason grade 6 ($P < 0.05$).

The expression of RPL22L1 and RPS21 in cell lines

Western blot was used to test the expression of RPL22L1 and RPS21 in PCa cell lines (PC3 and DU145). The results showed that the expressions of RPL22L1 and RPS21 were higher in PC3 cells line than in DU145 cells line ($P > 0.05$). As PC3 cells line had the higher expressions of RPL22L1 and RPS21, PC3 cells line was chosen for further investigation (Fig. 6a). To assess the roles of RPL22L1 and RPS21 in PC3 cell, their expressions were knocked down by transfection using lentivirus-RPL22L1/RPS21-shRNA. Then, western blot analysis revealed that protein expressions of RPL22L1 and RPS21 were significantly decreased in cell lines transfected with RPL22L1/RPS21-shRNA compared with the controls ($P < 0.05$, Fig. 6b).

RPL22L1 and RPS21 promote PC3 cell proliferation

To investigate whether RPL22L1 and RPS21 promote PC3 cell proliferation, CCK8 assay and colony formation assay were performed. The results showed that knockdown of

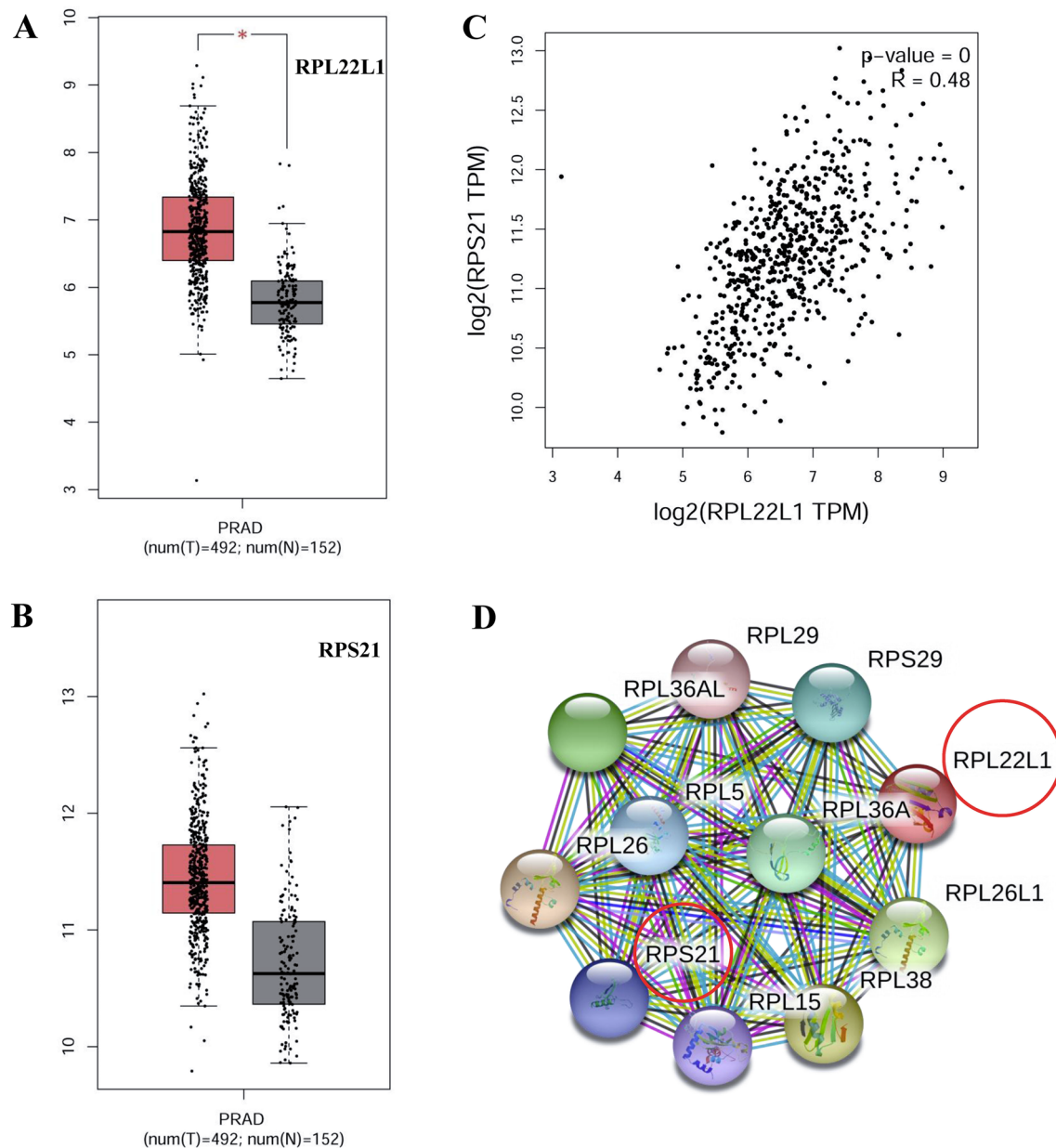


Fig. 1 Analysis of RPL22L1 and RPS21 by bioinformatics tool. **a** The expression of RPL22L1 from GEPIA analysis. **b** The expression of RPS21 from GEPIA analysis. **c** The correlation between RPL22L1

and RPS21 from GEPIA analysis. **d** The protein-protein interaction from STRING database analysis

RPL22L1/RPS21 significantly suppressed proliferation of PC3 cell ($P < 0.05$, Fig. 7a). Moreover, colony formation ability was remarkably decreased in PC3 cells of RPL22L1/RPS21 knockdown compared with the controls ($P < 0.05$, Fig. 7b). These results demonstrated that RPL22L1 or RPS21 promote PCa cell proliferation.

RPL22L1 and RPS21 promote PC3 cell migration and invasion

To determine whether RPL22L1 and RPS21 promote PC3 cell migration and invasion, wound-healing assay and transwell assay were carried out. The wound-healing

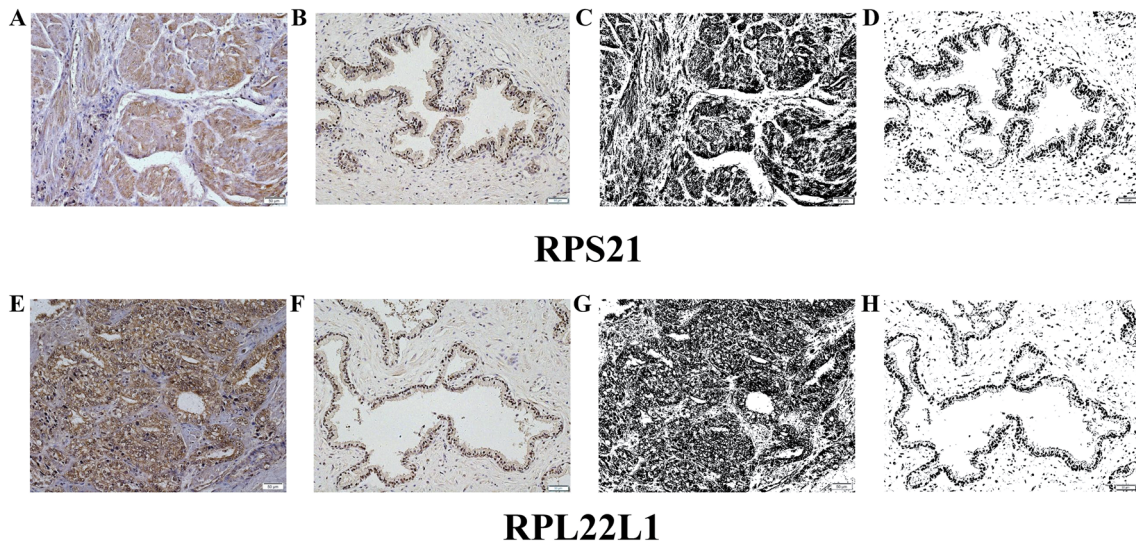


Fig. 2 The expression of RPL22L1 and RPS21 in PCa and normal prostate tissues. The expression of RPL22L1 and RPS21 were confirmed by IHC, and then the images were converted for quantification of the DAB signal by ImageJ software. **a** RPS21 of PCa; **b** RPS21

of control; **e** RPL22L1 of PCa; **f** RPL22L1 of control. Binary, the converted images (**c, d, g, h**) represented pixels that were positive for each representative antibody. Scale bars, 50 μ m. IHC immunohistochemistry, PCa prostate cancer; control: normal prostate tissues

Fig. 3 Expression analysis of DAB signal in PCa and normal prostate tissues. AF was calculated, and each bar represented the AF of a tissue core. Red represented the prostate cancer cores and green represented the normal prostate cores. **a** AF of RPL22L1; **b** AF of RPS21. AF area fraction; PCa prostate cancer

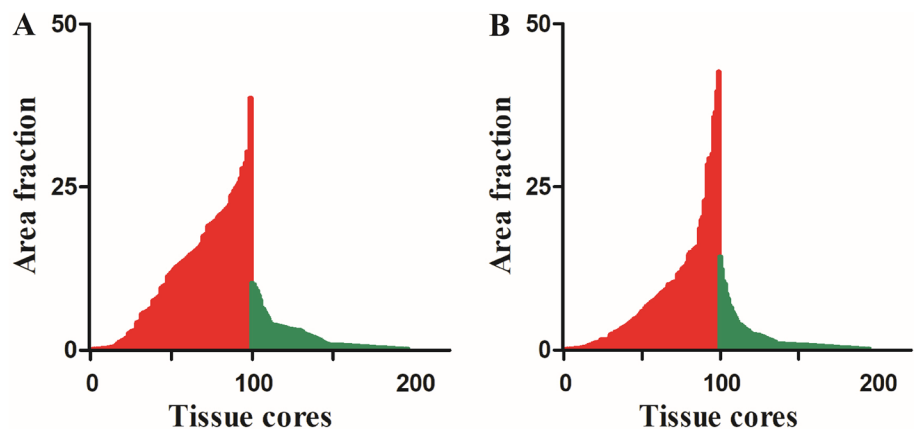
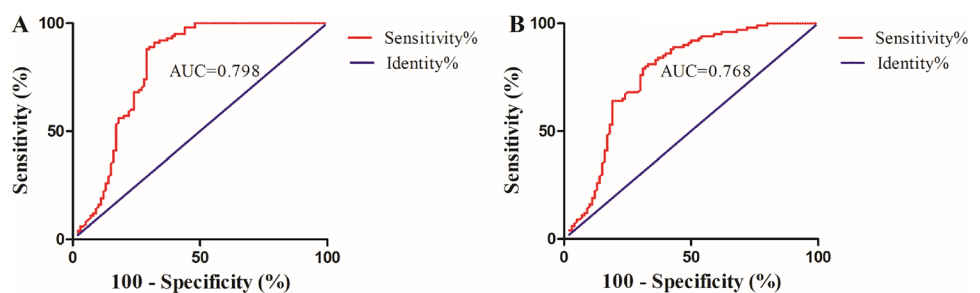


Fig. 4 ROC curves of RPL22L1 and RPS21 in PCa and normal tissues. ROC curves were prepared to verify if RPL22L1 and RPS21 might be potential biomarker of PCa. **a** ROC curve of RPL22L1; **b** ROC curve of RPS21. ROC receiver-operating characteristics, PCa prostate cancer



results revealed that the migration ability was significantly descended in PC3 cells of RPL22L1/RPS21 knockdown compared with the controls ($P < 0.05$, Fig. 8a). Meanwhile, the transwell results suggested that the invasion ability of

RPL22L1/RPS21 knockdown PC3 cells was diminished compared with the controls ($P < 0.05$, Fig. 8b). Taken together, these data demonstrated that RPL22L1 or RPS21 promote PCa cell migration and invasion.

Fig. 5 Changes in expression of RPL22L1 and RPS21 with Gleason grade. Box plots were created by Graphpad Prism software to show the changes in RPL22L1 and RPS21 expression with Gleason grade. **a** Changes in expression of RPL22L1 with Gleason grade; **b** Changes in expression of RPS21 with Gleason grade. * $P < 0.05$

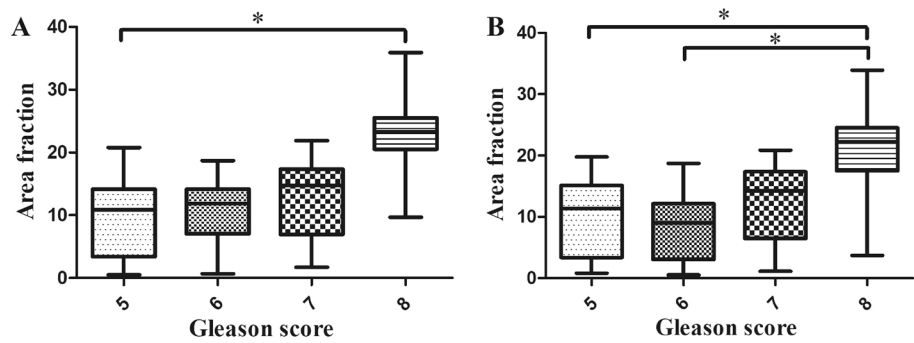
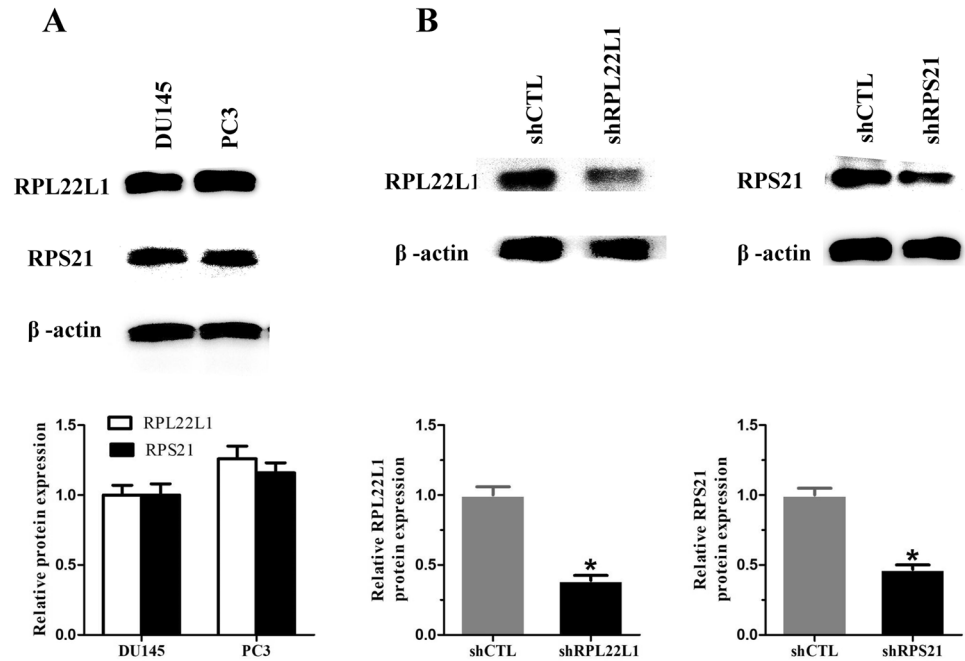


Fig. 6 Effective knockdown of RPL22L1 and RPS21 in PC3 cell. **a** The expression of RPL22L1 and RPS21 in PC3 cells line compared with the DU145 cells line. **b** PC3 cell was transfected using lentivirus-RPL22L1/RPS21-shRNA. Western blot was used to test the transfection efficiency. PCa: prostate cancer, shCTL: negative control shRNA; * $P < 0.05$. Error bars indicate SE



RPL22L1 and RPS21 inhibit PC3 cell apoptosis

Finally, we examined whether RPL22L1 and RPS21 affect PC3 cell apoptosis. The results of flow cytometry analysis showed that the apoptosis was notably increased in PC3 cells of RPL22L1/RPS21 knockdown compared with the controls ($P < 0.05$, Fig. 9). These results demonstrated that RPL22L1 or RPS21 inhibit PCa cell apoptosis.

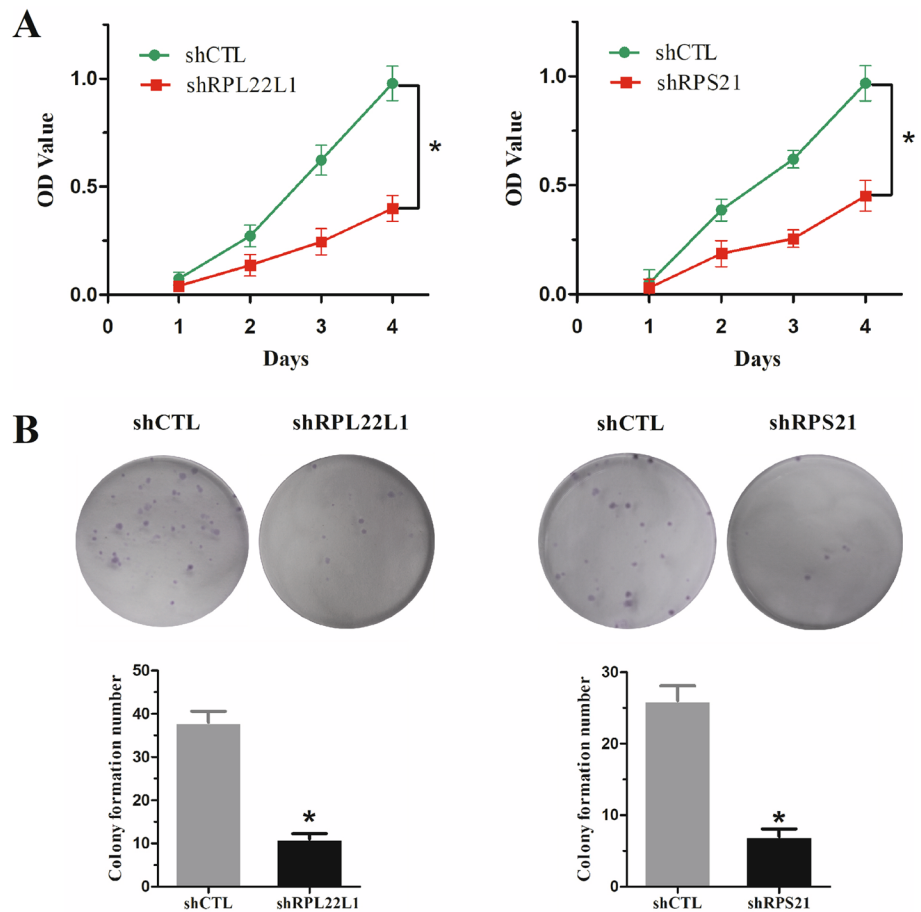
Discussion

In the present study, we investigated the potential of RPL22L1 and RPS21 as diagnostic and prognostic biomarkers for PCa. First, RPL22L1 and RPS21 were screened as the key molecular of PCa by bioinformatics analysis. Subsequently, the IHC of RPL22L1 and RPS21 were performed, and then the unbiased signal quantification was carried out. The results showed that the expression of RPL22L1 and

RPS21 exhibited significant differences between the PCa tissues and the normal prostate tissues. The further analysis showed that the expression of RPL22L1 and RPS21 were significantly higher in high Gleason grade than they were in low Gleason grade. Moreover, the results of in vitro studies revealed that RPL22L1 and RPS21 promote PCa cell proliferation, migration and invasion, and inhibit PCa cell apoptosis. Collectively, these data demonstrated that RPL22L1 and RPS21 exhibited higher expression in human cancerous prostate tissue, and involved in PCa cell proliferation and invasion.

RPL22L1, a component of the 60S subunit [21], was first identified in mouse brain [22]. O'Leary et al. reported that RPL22L1 was regulated by RPL22, and played an imported role in cell growth [23]. The research of Zhang et al. suggested that RPL22L1 was crucial for T cell development of zebrafish [24]. In addition, previous study showed that RPL22L1 could promotes ovarian cancer metastasis by inducing Epithelial-to-Mesenchymal Transition [25]. In

Fig. 7 RPL22L1 and RPS21 promote PC3 cell proliferation. **a** The cell viability of RPL22L1 and RPS21 knockdown cells was tested by CCK8 assays at different time points. **b** The colony formation assay of RPL22L1 and RPS21 knockdown cells was done. shCTL: negative control shRNA; * $P < 0.05$. Error bars indicate SE



our recent study, RPL22L1 and PRS21 were identified as hub genes involved in PCa by bioinformatics analysis [13]. Aside from these, little is known about the role of this protein in disease. In this study, we observed that the expression of RPL22L1 was raised significantly in human PCa tissue. Meanwhile, we also found that RPL22L1 expression was significantly upregulated in high Gleason grade PCa. ROC curve analysis showed that AUC value was 0.798, and LR value was 2.86. The AUC value over 0.5 indicated the matter measured would yield significant distinction between the two groups. Likewise, the LR value over 1.0 implied that the presence of the tested signal would be associated with the presence of disease [26]. Therefore, these data indicated that RPL22L1 might be a candidate diagnostic and prognostic biomarker for PCa. Furthermore, the results of in vitro studies showed that RPL22L1 could promote PCa cell proliferation, migration and invasion, and repress PCa cell apoptosis. This suggested that RPL22L1 could also be exploited as potential therapeutic target for PCa.

RPS21 is known as a component of the 40S subunit [27]. Little is known about the research on RPS21. Sun et al. demonstrated that expression of RPS21 was upregulated in HBV-associated human hepatocellular carcinoma (HCC) cell lines using semi-quantitative RT-PCR [28]. Elumalai et al.

reported that RPS21 expression was decreased by the treatment of doubly cyclometalated ruthenacycle 2 in the gastric carcinoma (AGS) cells [29]. Arthurs et al. found that expression of RPS21 was elevated in PCa tissue [15]. Likewise, we tested the expression of RPS21, and the results confirmed that RPS21 expression was also increased significantly in human PCa tissue. ROC curve analysis was performed, and the result showed that AUC value was 0.768, and LR value was 2.53. Further analysis indicated that the expression of RPS21 was also significantly upregulated in high Gleason grade PCa. Moreover, in vitro studies demonstrated that RPS21 could promote PCa cell proliferation, migration and invasion. These results indicated that RPS21 might be also a putative diagnostic and prognostic biomarker and potential therapeutic target for PCa.

As RPL22L1 and RPS21 are over-expressed in PCa tissues and PCa cells, we speculate that the change of these genes might also exist in circulating tumor cells. Detection of the expression of RPL22L1 and RPS21 in circulating tumor cells might contribute to early diagnosis of PCa. The relevant clinical study in this aspect will be further investigated. In addition, the molecular mechanism of RPL22L1 and RPS21 will be also explored to illustrate their role in PCa progression and metastasis.

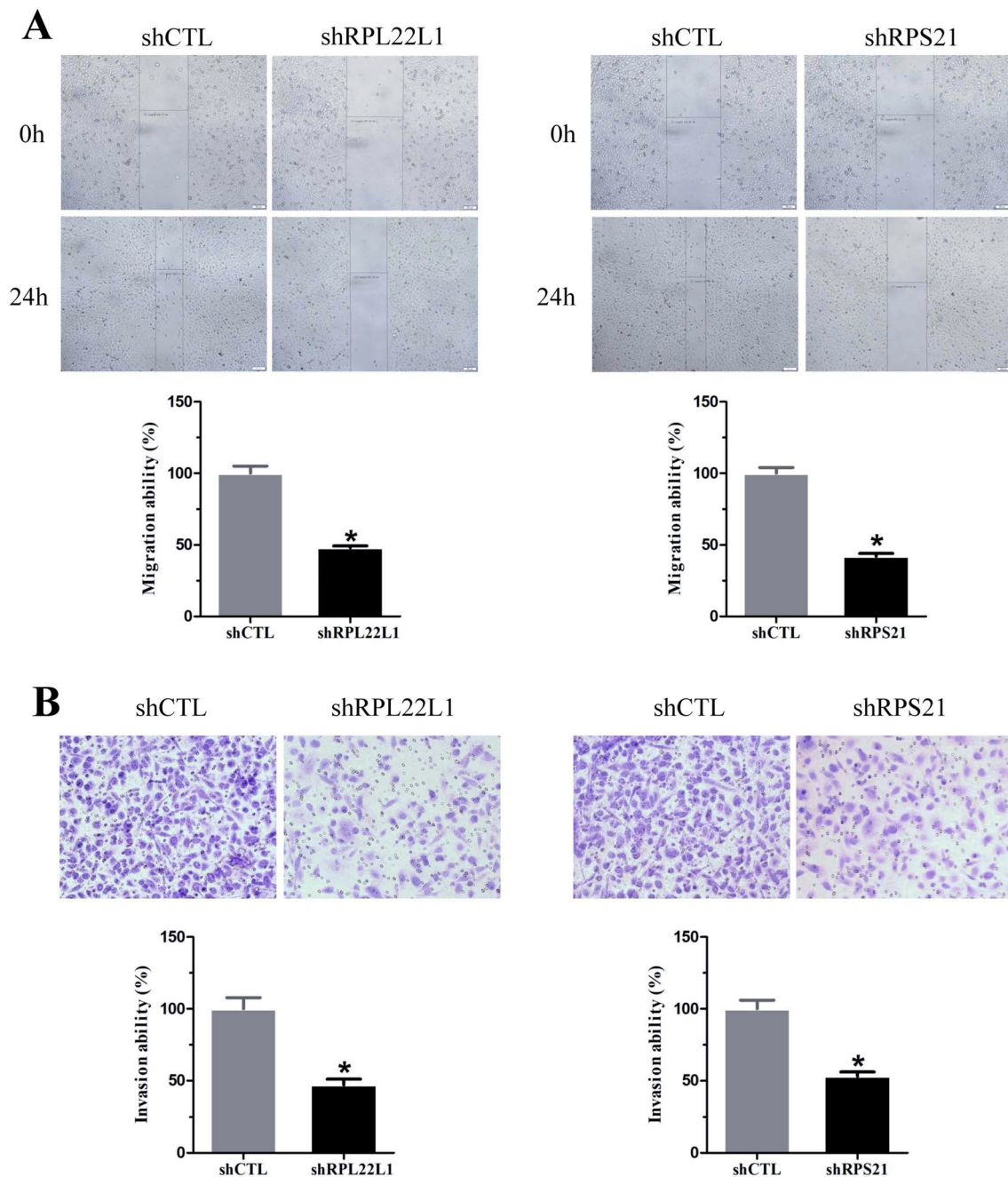


Fig. 8 RPL22L1 and RPS21 promote PC3 cell migration and invasion. **a** The wound-healing ability of RPL22L1 and RPS21 knockdown cells was determined at 24 h after seeding. **b** The invasion

ability of RPL22L1 and RPS21 knockdown cells was examined by transwell assays. shCTL: negative control shRNA; * $P < 0.05$. Error bars indicate SE

In conclusion, we demonstrated that the expression of RPL22L1 and RPS21 were significantly upregulated in human cancerous prostate tissue compared to the normal prostate tissue, and involved in PCa cell proliferation and

invasion. Our results suggested that RPL22L1 and RPS21 might be candidate diagnostic and prognostic biomarkers for PCa.

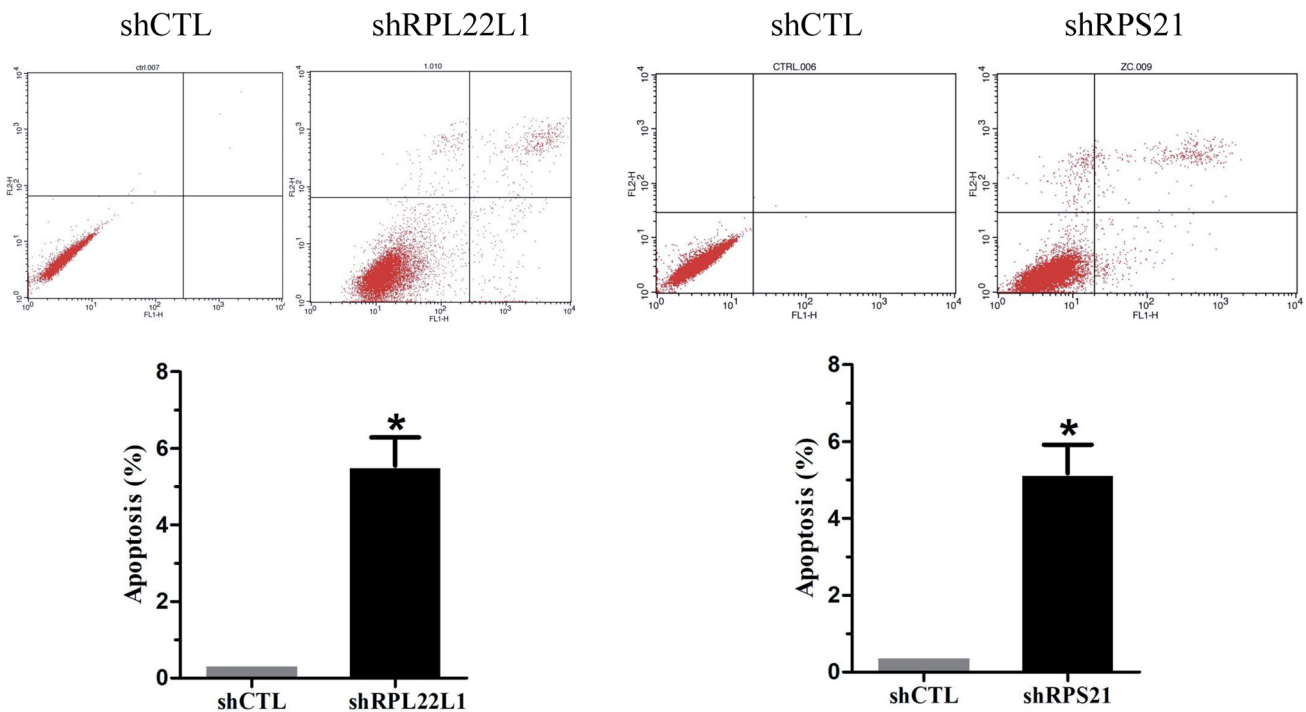


Fig. 9 RPL22L1 and RPS21 inhibit PC3 cell apoptosis. Flow cytometric assay was performed to analyze cell apoptosis of RPL22L1 and RPS21 knockdown cells. shCTL: negative control shRNA; * $P < 0.05$. Error bars indicate SE

Acknowledgements We thank Bo Lian for his technical assistance.

Funding The study was supported by Natural Science Foundation of Shandong Province (ZR2014CL034, ZR2018MC015), Medical and Health Development Plan of Shandong Province (2017WS058) and Research and Development Plan of University in Shandong Province (J18KA120).

Compliance with ethical standards

Conflict of interest The authors declare that they have no financial or competing interests.

Ethical approval This study was approved by the Research Ethics Committee of Weifang Medical University (Weifang, China). The procedures performed in present study were in accordance with the ethical standards of the institutional and/or national research committee and with the 1964 Helsinki declaration and its later amendments or comparable ethical standards.

Informed consent Informed consent was obtained from all individual participants included in the study.

References

1. Wang L, Song G, Chang X, Tan W, Pan J, Zhu X, et al. The role of TXNDC5 in castration-resistant prostate cancer— involvement of androgen receptor signaling pathway. *Oncogene*. 2015;34(36):4735.

2. Yan G, Ru Y, Wu K, Yan F, Wang Q, Wang J, et al. GOLM1 promotes prostate cancer progression through activating PI3K-AKT-mTOR signaling. *Prostate*. 2018;78(3):166–77.
3. Siegel RL, Miller KD, Jemal A. Cancer statistics, 2018. *CA Cancer J Clin*. 2018;60(5):277–300.
4. Siegel RL, Miller KD, Jemal A. Cancer statistics, 2017. *CA Cancer J Clin*. 2017;67(1):7–30.
5. Gadzinski AJ, Cooperberg MR. *Prostate Cancer Markers*. Genitourinary Cancers. New York: Springer; 2018. p. 55–86.
6. Fujita K, Nonomura N. Urinary biomarkers of prostate cancer. *Int J Urol*. 2018;25(9):770–9.
7. Thompson IM, Pauler DK, Goodman PJ, Tangen CM, Lucia MS, Parnes HL, Minasian LM, Ford LG, Lippman SM, Crawford ED, Crowley JJ, Coltman CA. Prevalence of prostate cancer among men with a prostate-specific antigen level 4.0 ng per milliliter. *Urologic Oncol Semin Orig Investig*. 2004;22(6):493.
8. Zhou X, Liao W-J, Liao J-M, Liao P, Lu H. Ribosomal proteins: functions beyond the ribosome. *J Mol Cell Biol*. 2015;7(2):92–104.
9. Pelletier J, Thomas G, Volarević S. Ribosome biogenesis in cancer: new players and therapeutic avenues. *Nat Rev Cancer*. 2018;18(1):51.
10. Lopez CD, Martinovsky G, Naumovski L. Inhibition of cell death by ribosomal protein L35a. *Cancer Lett*. 2002;180(2):195–202.
11. Wang Q, Yang C, Zhou J, Wang X, Wu M, Liu Z. Cloning and characterization of full-length human ribosomal protein L15 cDNA which was overexpressed in esophageal cancer. *Gene*. 2001;263(1):205–9.
12. Henry JL, Coggin DL, King CR. High-level expression of the ribosomal protein L19 in human breast tumors that overexpress erbB-2. *Can Res*. 1993;53(6):1403–8.

13. Fan S, Liang Z, Gao Z, Pan Z, Han S, Liu X, et al. Identification of the key genes and pathways in prostate cancer. *Oncol Lett.* 2018;16(5):6663–9.
14. Feng W, Zhou D, Meng W, Li G, Zhuang P, Pan Z, et al. Growth retardation induced by avian leukosis virus subgroup J associated with down-regulated Wnt/ β -catenin pathway. *Microb Pathog.* 2017;104:48–55.
15. Arthurs C, Murtaza BN, Thomson C, Dickens K, Henrique R, Patel HR, et al. Expression of ribosomal proteins in normal and cancerous human prostate tissue. *PLoS ONE.* 2017;12(10):e0186047.
16. Giuliano A, Swift R, Arthurs C, Marote G, Abramo F, McKay J, et al. Quantitative expression and co-localization of Wnt signalling related proteins in feline squamous cell carcinoma. *PLoS ONE.* 2016;11(8):e0161103.
17. You X, Wei L, Fan S, Yang W, Liu X, Wang G, et al. Expression pattern of Zinc finger protein 185 in mouse testis and its role in regulation of testosterone secretion. *Mol Med Rep.* 2017;16(2):2101–6.
18. Cheng Y, Wang K, Geng L, Sun J, Xu W, Liu D, et al. Identification of candidate diagnostic and prognostic biomarkers for pancreatic carcinoma. *EBioMedicine.* 2019;40:382–93.
19. Yang L, Zha T-Q, He X, Chen L, Zhu Q, Wu W-B, et al. Placenta-specific protein 1 promotes cell proliferation and invasion in non-small cell lung cancer. *Oncol Rep.* 2018;39(1):53–60.
20. Zhang L, Qi M, Feng T, Hu J, Wang L, Li X, et al. IDH1R132H promotes malignant transformation of benign prostatic epithelium by dysregulating MicroRNAs: involvement of IGF1R-AKT/STAT3 signaling pathway. *Neoplasia.* 2018;20(2):207–17.
21. Sugihara Y, Honda H, Iida T, Morinaga T, Hino S, Okajima T, et al. Proteomic analysis of rodent ribosomes revealed heterogeneity including ribosomal proteins L10-like, L22-like 1, and L39-like. *J Proteome Res.* 2010;9(3):1351–66.
22. Ballif BA, Cao Z, Schwartz D, Carraway KL, Gygi SP. Identification of 14-3-3 ϵ substrates from embryonic murine brain. *J Proteome Res.* 2006;5(9):2372–9.
23. O’Leary MN, Schreiber KH, Zhang Y, Duc A-CE, Rao S, Hale JS, et al. *v. PLoS Genet.* 2013;9(8):3708.
24. Zhang Y, Duc A-CE, Rao S, Sun X-L, Bilbee AN, Rhodes M, et al. Control of hematopoietic stem cell emergence by antagonistic functions of ribosomal protein paralogs. *Dev Cell.* 2013;24(4):411–25.
25. Wu N, Wei J, Wang Y, Yan J, Qin Y, Tong D, et al. Ribosomal L22-like1 (RPL22L1) promotes ovarian cancer metastasis by inducing epithelial-to-mesenchymal transition. *PLoS ONE.* 2015;10(11):e0143659.
26. Fawcett T. An introduction to ROC analysis. *Pattern Recogn Lett.* 2006;27(8):861–74.
27. Sato M, Kong CJ, Yoshida H, Nakamura T, Wada A, Shimoda C, et al. Ribosomal proteins S0 and S21 are involved in the stability of 18S rRNA in fission yeast, *Schizosaccharomyces pombe*. *Biochem Biophys Res Commun.* 2003;311(4):942–7.
28. Yoon SY, Kim J-M, Oh J-H, Jeon Y-J, Lee D-S, Kim JH, et al. Gene expression profiling of human HBV-and/or HCV-associated hepatocellular carcinoma cells using expressed sequence tags. *Int J Oncol.* 2006;29(2):315–27.
29. Elumalai P, Jeong YJ, Park DW, Kim DH, Kim H, Kang SC, et al. Antitumor and biological investigation of doubly cyclometalated ruthenium (ii) organometallics derived from benzimidazolyl derivatives. *Dalton Trans.* 2016;45(15):6667–73.

Publisher’s Note Springer Nature remains neutral with regard to jurisdictional claims in published maps and institutional affiliations.